

AD-A010 508

AN INVESTIGATION OF OBLIQUE PERFORATION OF
METALLIC PLATES BY PROJECTILES

J. Awerbuch, et al

Technion - Israel Institute of Technology

Prepared for:

Air Force Office of Scientific Research
European Office of Aerospace Research

March 1975

DISTRIBUTED BY:

NTIS

National Technical Information Service
U. S. DEPARTMENT OF COMMERCE

Best Available Copy

ADAO10508

REPORT NO. 63

March 1971

March 1971



SCIENTIFIC REPORT NO. 63
MARCH 1971
MATERIAL MECHANICS LABORATORY

ISRAEL INSTITUTE OF TECHNOLOGY
DEPARTMENT OF MATERIALS ENGINEERING
MATERIAL MECHANICS LABORATORY
HAIFA, ISRAEL

DDC
REF ID: A6010508
JUN 5 1975
R
D

AIR FORCE OFFICE OF SCIENTIFIC RESEARCH (AFOSR)
NOTICE OF TRANSMISSION TO AFOSR

THIS DOCUMENT CONTAINS INFORMATION OF A PRELIMINARY NATURE AND IS NOT TO BE USED FOR OFFICIAL PURPOSES WITHOUT THE WRITTEN PERMISSION OF THE AIR FORCE OFFICE OF SCIENTIFIC RESEARCH

Document No. 63

Reproduced by
NATIONAL TECHNICAL
INFORMATION SERVICE
U.S. Department of Commerce
Springfield, VA 22151

Scientific Report No. 63
SOAR, USAF
Grant AFOSR-76-25076

Approved for public release;
Distribution unlimited.

Best Available Copy

REPORT DOCUMENTATION PAGE		READ INSTRUCTIONS BEFORE COMPLETING FORM
1. REPORT NUMBER AFOSR - TR - 75 - 0717	2. GOVT ACCESSION NO.	3. RECIPIENT'S CATALOG NUMBER
4. TITLE (and Subtitle) AN INVESTIGATION OF OBLIQUE PERFORATION OF METALLIC PLATES BY PROJECTILES		5. TYPE OF REPORT & PERIOD COVERED INTERIM 1974-1975 Report 6
7. AUTHOR(s) J AWERBUCH S R BODNER		6. PERFORMING ORG. REPORT NUMBER MED Report No 48
9. PERFORMING ORGANIZATION NAME AND ADDRESS TECHNION - ISRAEL INSTITUTE OF TECHNOLOGY DEPARTMENT OF MATERIALS ENGINEERING HAIFA, ISRAEL		8. CONTRACT OR GRANT NUMBER(s) AFOSR 74-2607
11. CONTROLLING OFFICE NAME AND ADDRESS AIR FORCE OFFICE OF SCIENTIFIC RESEARCH/NA 1400 WILSON BOULEVARD ARLINGTON, VIRGINIA 22209		10. PROGRAM ELEMENT, PROJECT, TASK AREA & WORK UNIT NUMBERS 681307 9782-04 61102F
12. REPORT DATE March 1975		13. NUMBER OF PAGES 39
14. MONITORING AGENCY NAME & ADDRESS (if different from Controlling Office)		15. SECURITY CLASS. (of this report) UNCLASSIFIED
16. DISTRIBUTION STATEMENT (of this Report) Approved for public release; distribution unlimited.		15a. DECLASSIFICATION/DOWNGRADING SCHEDULE
17. DISTRIBUTION STATEMENT (of the abstract entered in Block 20, if different from Report)		
18. SUPPLEMENTARY NOTES		
19. KEY WORDS (Continue on reverse side if necessary and identify by block number) BALLISTICS, TERMINAL DYNAMIC PLASTICITY PERFORATION PENETRATION IMPACT (OBLIQUE) ARMOR		
20. ABSTRACT (Continue on reverse side if necessary and identify by block number) An experimental and analytical study was performed on the mechanics of oblique perforation of projectiles in metallic plates. The purpose was to determine the dependence of the velocity drop on the angle of impact for prescribed mechanical and physical properties of the projectile and the target plate. The ballistic experiments were carried out with 0.22 inch caliber lead bullets on target plates of commercially pure aluminum and analuminum alloy which ranged from 2.0 to 6.0 mm in thickness. Transient measurements were taken which included high speed photographs of the perforation process. The theoretical model that had been		

UNCLASSIFIED

SECURITY CLASSIFICATION OF THIS PAGE(When Data Entered)

developed previously by the authors for the case of normal perforation was modified to include the effects of the angle of impact. The experimental observations for the present test conditions indicate that the only essential modification to the analysis is the use of the total projectile path as the effective target plate thickness. The comparison of the results shows reasonably good agreement between experiments and theory.

UNCLASSIFIED

11
SECURITY CLASSIFICATION OF THIS PAGE(When Data Entered)

GRANT AFOSR - 74 - 2607B

March 1975

SCIENTIFIC REPORT NO. 6

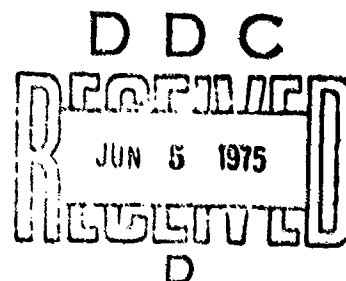
AN INVESTIGATION OF OBLIQUE
PERFORATION OF METALLIC PLATES BY PROJECTILES

by

J. AWERBUCH AND S.R. BODNER

MED Report No. 48

Material Mechanics Laboratory
Department of Materials Engineering
Technion - Israel Institute of Technology
Haifa, Israel



The research reported in this document has been supported in part by the AIR FORCE OFFICE OF SCIENTIFIC RESEARCH under Grant AFOSR-74-2607B, through the European Office of Aerospace Research (EOAR), United States Air Force.

DISTRIBUTION STATEMENT A

Approved for public release;
Distribution Unlimited

1-

AN INVESTIGATION OF OBLIQUE
PERFORATION OF METALLIC PLATES BY PROJECTILES

by

J. Awerbuch¹ and S.R. Bodner²

Abstract

An experimental and analytical study was performed on the mechanics of oblique perforation of projectiles in metallic plates. The purpose was to determine the dependence of the velocity drop on the angle of impact for prescribed mechanical and physical properties of the projectile and the target plate. The ballistic experiments were carried out with 0.22 inch caliber lead bullets on target plates of commercially pure aluminum and an aluminum alloy which ranged from 2.0 to 6.0 mm in thickness. Transient measurements were taken which included high speed photographs of the perforation process. The theoretical model that had been developed previously by the authors for the case of normal perforation was modified to include the effects of the angle of impact. The experimental observations for the present test conditions indicate that the only essential modification to the analysis is the use of the total projectile path as the effective target plate thickness. The comparison of the results shows reasonably good agreement between experiments and theory.

¹Lecturer, Department of Materials Engineering
Technion - Israel Institute of Technology
presently, N.R.C. Research Associate, USAF Materials Lab, WPAFB, Ohio, U.S.A.

²Professor, Department of Materials Engineering,
Technion - Israel Institute of Technology

Introduction

The problem of oblique perforation can generally be separated into three ranges of impact angles. The first range of complete perforation extends to some angle α_1 at which the projectile is stopped by the target plate. The value of α_1 depends on many parameters such as the mechanical and physical properties of the target and projectile and on the impact velocity. The second range of angles of impact is for $\alpha > \alpha_1$ where the projectile continues to be stopped by the target in which it is imbedded, i.e. it does not ricochet. Generally, this is a small range, 1° to 5° . In the third range of large angles of impact, the projectile ricochets from the target. It is the first range of angles of impact that is studied in this paper.

An analysis of the mechanics of normal perforation of metallic plates by projectiles at ordnance velocities has been developed [1] from which the post perforation velocity can be calculated. This analysis also predicts the contact time and force-time history. An extensive experimental program had been performed as part of the overall investigation to provide detailed information on the physics of the perforation process [2]. Calculations based on the theory [1] were found to be in reasonably good agreement with the experimental results [2].

In the present report, the theory of normal perforation [1] is modified to include the effect of the angle of impact. Results of ballistic experiments are reported which were carried out with 0.22 inch caliber lead bullets

obliquely perforating aluminum plates. The purpose of the experimental program was to assist the development of the analysis by giving information on the physical aspects of the oblique perforation process and to provide results for comparison purposes.

Previous Investigations

Most of the experimental and theoretical investigations that have been published on the subject of projectile perforation are limited to the case of normal penetration of projectiles, and relatively little has been published on the problem of oblique perforation. In a study by Zener and Peterson [3], the authors conclude that the effect of the angle of impact on the projectile's residual velocity is primarily due to the increase of the projectile path in the target plate according to the relationship: $h' = h / \cos(\alpha + \Delta\alpha)$. The quantity $\Delta\alpha$ is the change of the angle of penetration due to the action of the transverse force acting on the projectile during initial contact. In another study, Recht & Ipson [4] developed an energy analysis from which the post perforation velocity could be calculated provided the minimum perforation velocity is known. In their work, they examined the total angular change in direction of the projectile as it passes through the plate. Recht & Ipson [4] assumed that the ejected plug and the projectile move in the same direction and with the same velocity at the end of the perforation process. The calculation of the residual velocity is based on an analysis developed for the case of normal perforations in which only the momentum in the direction of movement is considered.

These authors consider the plug to be elliptical having a major diameter $D_p / \cos \alpha$ and mass $M_p / \cos \alpha$ where D_p and M_p are the plug's diameter and mass for the normal impact case.

A large number of tests on crater formation at very high impact velocities have been performed by many investigators concerned with hypervelocity impact. For example, a series of ballistic experiments at oblique angles were carried out by Summers [5]. The target plates were of copper and the projectiles were 1/8 inch diameter copper spheres moving at muzzle velocities of 7,000 ft/sec and 11,000 ft/sec. In that investigation, the effect of the angle of impact on the depth of penetration was studied and it was found that the component of velocity parallel to the target surface does not contribute significantly to the target penetration for a range of angles of obliquity up to 40° for the lower impact velocity and up to 50° for the higher impact velocity.

In the relatively low velocity range, Goldsmith & Gunnigham [6] carried out oblique impact experiments on steel beams to study the crater geometry produced by the impact of 1/2 inch diameter steel spheres at initial velocities ranging from 30-150 ft/sec. The experimental results showed that the crater depth, as well as the magnitude of the deflection of the center of the beam, varied as the cosine of the angle of impact.

Analysis

The experimental observations (discussed in the following sections) indicate that, for the projectiles and target plates employed in these tests, the mechanism of oblique perforation is essentially the same as for normal impact. On this basis, the model and mathematical formulation that was developed for the case of normal perforation [1] could also serve for the oblique case. Although this assumption, i.e., that both cases can be treated in the same manner, may not hold for all types of projectiles and target plates, it seems to be a reasonable method of first approximation to the general problem of oblique perforation.

In the analysis of normal perforation, [1], the process is divided into three interconnected stages. The first, compressive, stage involves inertial and compressive forces acting on the projectile. A shearing force arises in the second stage of incipient plugging which also includes the other forces. The shearing force is due to the relative deformation of target material that is accelerated by the projectile in relation to the target plate. Due to the addition of target material, a changing effective mass of the projectile is considered in the first and second stages. The second stage ends when all target material forward of the projectile (the plug) moves at the same velocity as the projectile. In the subsequent third stage of plug ejection, only the shearing force acts on the plug's circumference and along its length until the failure strain in shear is reached.

The compressive and inertial forces of the first stage of oblique perforation are taken to act in the direction of the projectile path which is that of the initial velocity vector. These forces are given in [1] as $F_c = \sigma_c A$ and $F_i = (1/2)K\rho AV^2$ where A is the cross sectional area of the cavity on a plane normal to the projectile path and therefore includes the effect of flattening of the projectile. For the oblique impact case, A can be taken as $A_1 \cos\alpha$ where A_1 is the entrance cavity area on the face of the plate. It is observed experimentally that A_1 is generally elliptical in form and that the minor axis is the diameter of the cylindrical cavity on the plane normal to the path. A good approximation to the length of the major axis is the minor axis divided by $\cos\alpha$. The area A would not, in general, be the same as that for normal impact since the flattening of the projectile may depend on α , although the present test results do indicate that the observed values of A are close to those of the corresponding normal impact case.

On considering the mechanism for oblique impact to be the same as for normal impact, the equation of motion for the first stage would be the same as Eq.(10) of [1] using A in place of A_1 . The coordinate x is then the distance along the projectile path, and an effective mass of projectile is considered in the same manner as in [1]. The first stage ends when x reaches $h'-b'$ where b' is the plug thickness and h' is $h/\cos\alpha$. An important observation of the experiments on normal impact [2] was that the plug thickness to plate thickness ratio b/h was almost constant for a given projectile and

target material over a wide range of thickness and initial velocities. It would therefore follow that to good approximation $(b'/h') = (b/h)$ and the second stage would commence when $x = (h-b)/\cos\alpha$.

For the second stage of the perforation process, the same equation of motion as for normal impact would hold, eq. (16) of [1], in which x is again the projectile displacement along the path and h and b would be replaced by h' and b' . The diameter D_2 and area A_2 refer in this case to the second stage cavity cross section in the plane normal to the projectile path. These quantities are not necessarily the same as for normal impact due to the influence of α on the projectile flattening effect.

Similar considerations hold for the third stage of perforation. The effective mass is then the projectile mass plus the total mass of target material ejected from the cavity namely, $m_0 + \rho \bar{A} h'$, where \bar{A} is the average cavity area on planes normal to the path. If \bar{A}' is the average cavity area in the plane of the plate and, as noted previously, $\bar{A} = \bar{A}' \cos\alpha$, then the total ejected target mass (plug plus fragments) is $\rho \bar{A}' h$.

The form of the equations for oblique perforation would therefore reduce to those of normal impact with an effective target thickness of $h' = h/\cos\alpha$ if the projectile path remained unchanged. A parameter in these equations is the cross sectional area of the cavity on planes normal to the path and this should be compared to that for normal impact for the same plate thickness. It is convenient experimentally to determine the cavity area from the entrance and exit openings in the plane of the target

plate. The experimental results on oblique impact indicate that the areas of these openings multiplied by $\cos\alpha$ agreed with those for normal impact for the same actual plate thickness and this result was used in the calculations. The oblique impact conditions, therefore, do not exactly correspond to those for normal impact on a plate of thickness h' since the cavity areas would not be exactly the same.

In actual fact, changes in the path of the projectile do occur and these can be of importance for relatively hard target plates and large impact angles. This effect, however, is not considered in the present treatment of the problem. Another effect not accounted for is that the plug ejects normal to the target plate rather than along the projectile path and has a rotational velocity, but this can be shown to have a small influence on the terminal velocity of the projectile.

It is noted that the terminal velocity is not a linear function of the initial velocity and of the target thickness. The same results would therefore not be obtained if the oblique perforation problem were reduced to that of normal perforation by using only the normal component of the initial impact velocity.

Experimental Procedure and Results

(a) Experimental Procedure.

The tests were performed in a ballistic range which provided for measurement of the initial and post-perforation velocities and high speed photography of the projectile. A detailed description of the test procedure is given in [2]. The geometrical parameters of the cavity, i.e., entrance and exit shapes, were measured after each test.

In order to obtain more information on the process of oblique perforation, the photographic equipment described in [2] was modified for multiple (triple) exposures at prescribed time intervals. Three stroboscopes (General Radio Types 1531, 1538A, and 1539) and auxiliary equipment were combined with three delay units for this purpose.

The projectiles were 0.22 inch caliber lead bullets with a muzzle velocity of 380-400 m/sec. Target plates were commercially pure aluminum (1100-H14) and aluminum alloy (6061-T6). The plate dimensions were 250x250 mm and ranged from 2.0 to 6.0 mm thick. Generally 3 tests were performed for each angle of impact and plate thickness. For large angles of impact - close to the ballistic limit - more tests were performed since the reproducibility of the results was not as good. In this range of angles of impact, the final velocity is sensitive to all the parameters and depends critically on the exact angle of impact and on the mechanical properties of the target material. The accuracy in determining the angle of impact is $\pm 1^\circ$.

(b) Experimental Results

The test results for the dependence of the velocity drop on the angle of impact are shown in Figs. 1 and 2 for the two target materials. It is noted that the effect of the angle of impact is small for a range of angles, while beyond this range the velocity drop increases rapidly for small changes in the impact angle. For example, in Fig. 1 for the 2mm plate, the effect of α is small for $\alpha < 50^\circ$, becomes large for $\alpha > 50^\circ$, and the projectile is stopped at $\alpha = 75^\circ$. This effect seems to be due to the sensitivity of the residual velocity near the ballistic limit on the target thickness which is magnified by the $\cos\alpha$ factor.

Figs. 3 and 4 show typical cross sections of the cavities of target plates that were perforated at various angles of impact. For commercially pure aluminum, Fig. 3, the angle of the axis of perforation was essentially straight and the same as the angle of impact. For the aluminum alloy plates, the axis was fairly straight but there was a deviation from the original direction. The theoretical predictions are, in fact, not as good for the aluminum alloy plates at large angles of impact as they are for the pure aluminum plates which seems to be partly due to this effect.

The contours of the entrance and exit openings in the plate had elliptical shapes with the major axis increasing with the angle of impact. The diameters of the openings were measured and the areas calculated based on the contours being exact ellipses. Results for the average of the entrance and exit opening areas as a function of α are shown in Figs. 5 and 6 for the various target plates.

The average areas multiplied by $\cos \alpha$ are also plotted, and the results are almost independent of α and close to the values corresponding to normal impact, $\alpha = 0$.

Figs. 7 and 8 show sequences of flash photographs at different times after impact. The individual photographs correspond to separate tests, and the times indicated are approximate due to variations in the initial velocities. Although the plug generally leaves the plate normal to the plate surface, the process of plug development is along the projectile path which can be seen by carefully superimposing successive photographs. The bulge at the rear of the plate appears during or after the third stage while the important second stage of plug formation cannot be easily visualized from the photographs. Some indication of this process can be obtained by careful measurements of the direction of growth of the bulge.

Multiple exposure photographs of the post perforation situation, Fig. 9, show that the projectile continues along its original path for the pure aluminum plates but deflects slightly for the aluminum alloy plates. In both cases, the plug is ejected normal to the plate except for conditions very close to the ballistic limit. It is also seen that the plug rotates as well as translates and an estimate of the rotational velocity can be obtained from the photographs.

Numerical results deduced from the multiple exposure photographs for particular target plates are listed in Table 1. Listed for each case are the residual translational velocity of the projectile and the translational and angular velocity of the plug. It is noted that the angular velocity is

of the order of 10^4 rad/sec. and has a maximum at a particular angle of impact. The translational velocity of the plug is close to the terminal velocity of the projectile at small angles of impact but decreases more rapidly for larger angles. This seems to be due, in part, to the transfer of part of the kinetic energy of uniform motion into rotational energy.

Discussion of Results

The results in Fig. 5 and 6 show that the cavity areas on planes normal to the projectile path are reasonably close to those obtained for normal impact for the same plate thickness. For commercially pure aluminum, the agreement is much closer than for the aluminum alloy, but it is still reasonable in the latter case. The post test examinations showed that the cavity axes approximately coincide with the initial impact directions for most of the cases. These observations indicate that the analysis of [1] can be applied to the present test results by replacing h and b in the equations by $h/\cos\alpha$ and $b/\cos\alpha$ respectively and by using results from normal impact tests for the cavity area normal to the projectile path.

Comparisons of theoretical predictions based on the above modifications of [1] with experimental results are shown in Figs. 10 to 15. The agreement between the sets of results for the commercially pure aluminum tests plates is fairly good and could be expected since the conditions for the applicability of the analysis are well realized physically. On the other hand, the assumptions in the analysis of constancy of the cavity

axis with the impact direction and equality of the cavity area with the equivalent normal impact case are less fulfilled for the tests on the harder aluminum alloy plates. The agreement is less good for these tests at the higher impact angles (close to the ballistic limit) where those effects would be more important.

The calculations were based on experimentally measured values of the entrance and exit opening areas, plug length b' , and shear zone width e (see [1]) for the various test conditions. As in [2], the average cavity area was used in the equations for all the stages of perforation. Since the ends of the ejected plugs were not fully flat, an average plug length was measured and used. The average values of b'/h' were found to be fairly constant for each material and essentially the same as those obtained in the normal impact tests [2]. The width of the shear zone e , which enters the equations of motion for the second and third stages, is not a sensitive parameter. It was assumed to be constant for all the plate thicknesses and the same as for normal impact.

Another parameter in the equations is the material viscosity at high shearing rates, μ , which was also taken to be the same as for normal impact conditions. The values of the parameters e and μ for aluminum are given in [2].

A factor not considered in the analysis is the non-symmetrical nature of the mechanism of separation of the plug from the plate. As seen from the high speed photographs, separation does not occur simultaneously around the circumference of the exit opening. After separation initially occurs

over part of the plug - target interface, the opposite side remains in contact for some time. This implies that the shearing stresses acting on the projectile during the third stage of perforation are not symmetrically distributed around the projectile. These stresses would be important under conditions close to the ballistic limit which is where the theoretical predictions of the analysis are less accurate.

A related effect not considered in the analysis is the "tearing" force which acts on the plug in the final stages of separation from the plate. The force is a factor in the transformation of the uniform motion of the plug along the projectile path to a motion normal to the plane of the plate combined with a rotation. The effect of this rotation on the terminal velocity of the projectile could be estimated from an analysis of the distribution of kinetic energy among the various components following perforation. That is, a reduction of kinetic energy of the projectile is required by the kinematic conditions to account for the rotational energy of the plug. Calculations of the reduction of the terminal velocity of the projectile due to plug rotation have been made and indicate that the effect is very small for the cases under consideration. The effects of the terminal non-symmetrical shearing and tearing forces are probably of some importance for the stronger target materials under conditions near the ballistic limit, but they are difficult to evaluate.

Conclusions

A simple modification of the analysis for normal perforation of plates by projectiles appears to give reasonably good predictions of terminal velocities for oblique impact tests on pure and 6061-T6 alloy aluminum target plates. The modification involves replacing the plate thickness by an effective thickness corresponding to an undeviated projectile path and considering the cavity area along the path to be the same as for normal impact for the actual plate thickness.

The basic analysis could, in principle, be adopted to cases where the projectile path does change direction and the cavity area normal to the path does vary with the angle of impact. In these cases, however, experimental measurements for these effects would be required for use in the computations.

The results show that the angle of impact has a small effect on the velocity drop over a range of angles. The influence of the impact angle becomes large near the ballistic limit condition.

For the present tests, the post perforation velocity vector of the projectile did not deviate substantially from the initial vector. Differences were greatest for the thicker aluminum alloy plates at the large impact angles. The plugs tended to be ejected normal to the plate surface with a rotational velocity induced by the tearing forces during final separation.

Acknowledgements

The authors wish to thank Mr. S. Peled, and Mr. Y. Avidor for their technical assistance in the construction of the ballistic range, and Mr. N. Bareket for his contributions to the development and operation of the electronic and photographic facilities. The assistance of Mr. I. Mermelstein in the performance of the tests is gratefully acknowledged.

REFERENCES

- [1]. J. Awerbuch and S.R. Bodner, Analysis of the mechanics of perforation of projectiles in metallic plates, Int. J. of Solids & Structures, 10, 671-684 (1974).
- [2]. J. Awerbuch and S.R. Bodner, Experimental investigation of normal perforation of projectiles in metallic plates, Int. J. of Solids & Structures, 10, 685-699 (1974).
- [3]. C. Zener and R.E. Peterson, Mechanics of armor penetration, Watertown Arsenal Report No. 710/492 (1943).
- [4]. R.F. Recht and T.W. Ipson, Ballistic perforation dynamics, J. Appl. Mech. 30, 384-390 (1963).
- [5]. J.L. Summers, Investigation of high speed impact: Regions of impact at oblique angles, NASA, TN D-94, (1959).
- [6] W. Goldsmith and D.H. Cunningham, Kinematic phenomena observed during the oblique impact of a sphere on a beam, J. Appl. Mech. 23, 612-616 (1956).

TABLE 1

Experimental Results of Projectile Impact and Postperforation Velocities,
Plug Velocities and Angular Rotations

Target Material	Thickness (mm)	Angle of Impact	Projectile Impact Velocity (m/sec)	Projectile Residual Velocity (m/sec)	Plug Velocity (m/sec)	Plug Angular Velocity (Rad/sec $\times 10^4$)
1100-H14	5	0°	394	271	271	0
		10°	391	268	268	0
		20°	388	247	214	1.26
		30°	383	218	156	1.83
		35°	393	208	91	1.15
		40°	382	170	0	0.12
		45°	389	0	0	0
1100-H14	6	0°	388	206	206	0
		10°	378	184	179	0.27
		20°	384	176	165	0.95
		30°	386	132	52	1.32
		35°	381	161	56	0
6061-T6	3	0°	384	310	310	0
		10°	388	308	303	1.15
		20°	385	284	214	1.55
		30°	375	270	154	4.50
		35°	383	262	96	3.30
		40°	382	178	0	0

List of Captions

- Fig. 1 - Experimental velocity drop of 0.22 in. caliber lead bullets perforating commercially pure aluminum plates of different thicknesses versus angle of impact (line indicates trend).
- Fig. 2 - Experimental velocity drop of 0.22 in. caliber lead bullets perforating aluminum alloy 6061-T6 plates of different thicknesses versus angle of impact (line indicates trend).
- Fig. 3 - Cross sections of commercially pure aluminum plates of different thicknesses after perforation by 0.22 in. caliber lead bullets at different angles of impact.
- Fig. 4 - Cross sections of aluminum alloy 6061-T6 plates of different thicknesses after perforation by 0.22 in. caliber lead bullets at different angles of impact.
- Fig. 5 - Dependence of the average cavity area on the angle of impact for commercially pure aluminum target plates of different thicknesses after perforation by 0.22 in. caliber lead bullets.
- Fig. 6 - Dependence of the average cavity area on the angle of impact for aluminum alloy 6061-T6 target plates of different thicknesses after perforation by 0.22 in. caliber lead bullets.
- Fig. 7 - Photographic sequence showing the oblique perforation process of 0.22 in. caliber lead bullets in commercially pure aluminum plate 5.0 mm thick ($\alpha=30^\circ$).

List of Captions (continued)

- Fig. 8 - Photographic sequence showing the oblique perforation process of 0.22 in. caliber lead bullets in aluminum alloy 6061-T6 plate 3.0 mm thick ($\alpha=30^\circ$).
- Fig. 9 - Multiple exposure photographs of 0.22 in. caliber lead bullets and plugs after perforation of aluminum plates (1100-H14, and 6061-T6).
- Fig. 10 - Projectile velocity drop versus angle of impact for 0.22 in. caliber lead bullet perforating commercially pure aluminum plate 2.0 mm thick.
- Fig. 11 - Projectile velocity drop versus angle of impact for 0.22 in. caliber lead bullet perforating commercially pure aluminum plate 4.0 mm thick.
- Fig. 12 - Projectile velocity drop versus angle of impact for 0.22 in. caliber lead bullet perforating commercially pure aluminum plate 5.0 mm thick.
- Fig. 13 - Projectile velocity drop versus angle of impact for 0.22 in. caliber lead bullet perforating aluminum alloy 6061-T6 plate 2.0 mm thick.
- Fig. 14 - Projectile velocity drop versus angle of impact for 0.22 in. caliber lead bullet perforating aluminum alloy 6061-T6 plate 3.5 mm thick.
- Fig. 15 - Projectile velocity drop versus angle of impact for 0.22 in. caliber lead bullet perforating aluminum alloy 6061-T6 plate 5.0 mm thick.

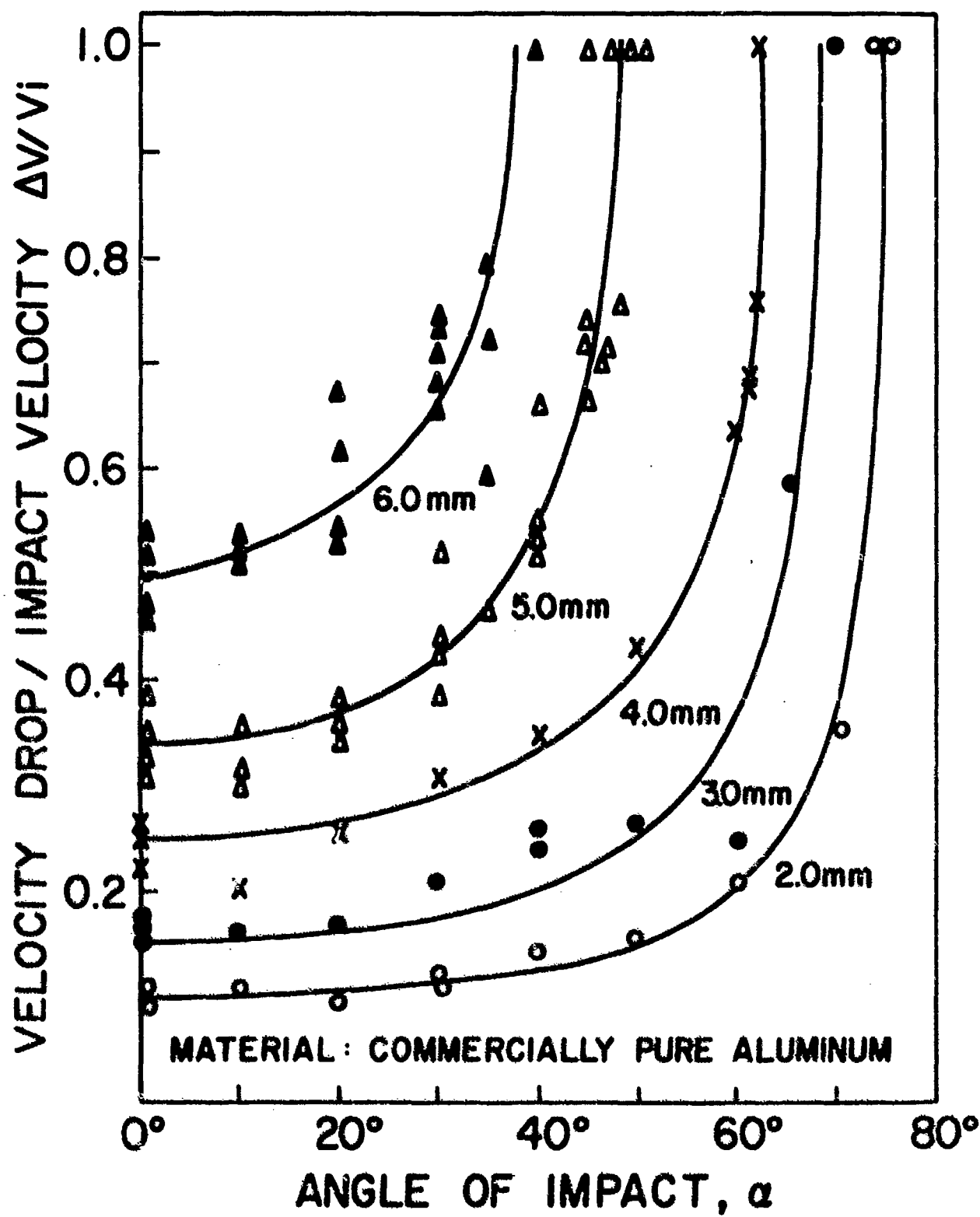


Fig.1

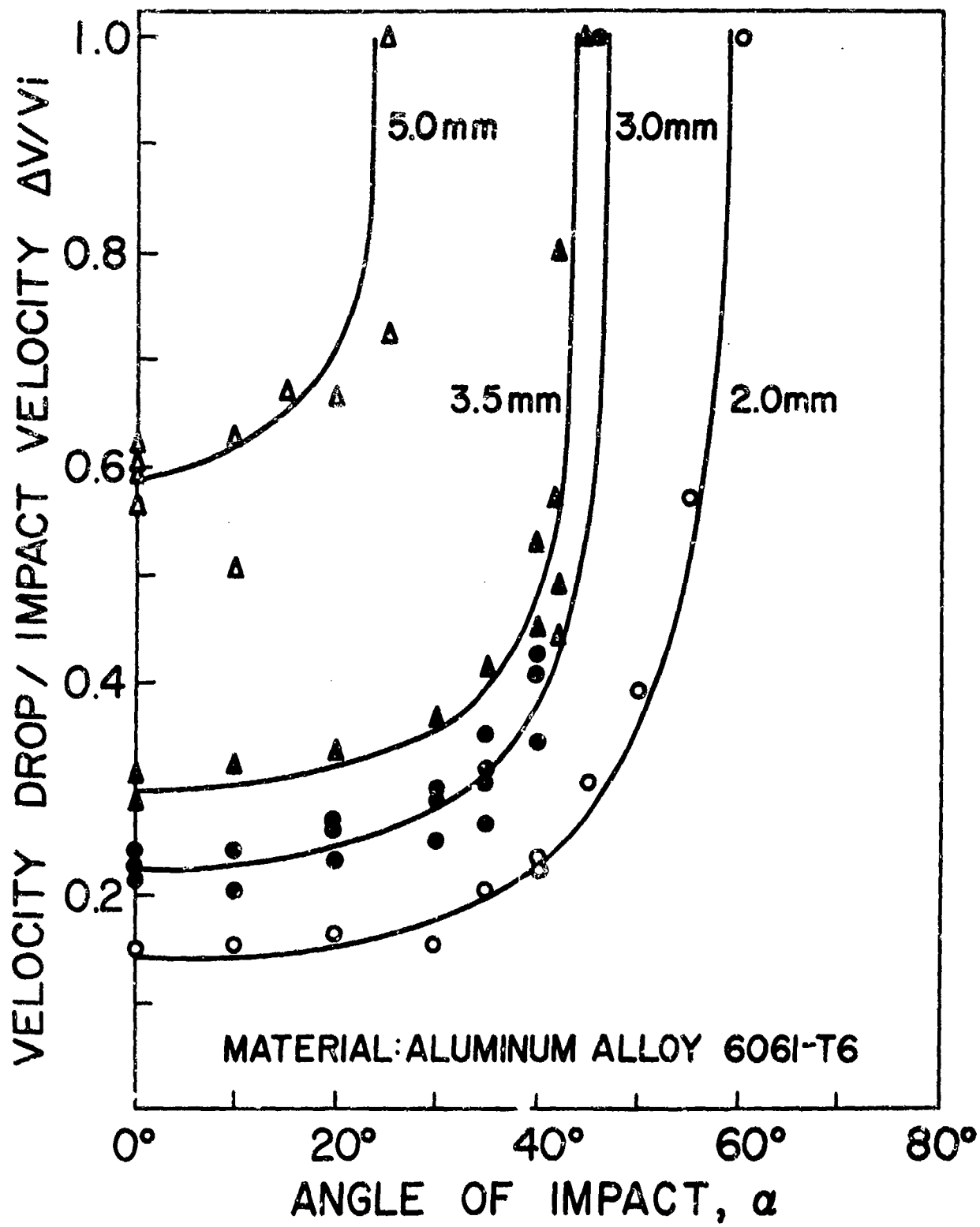
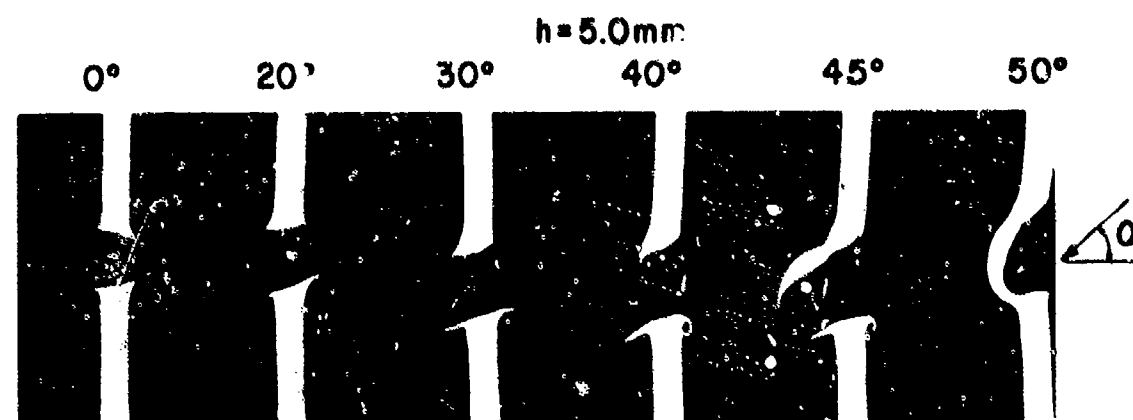
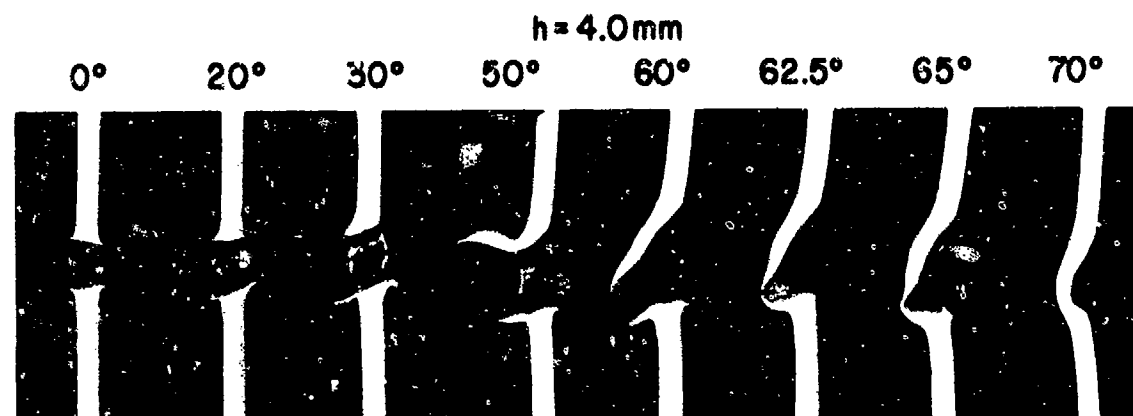
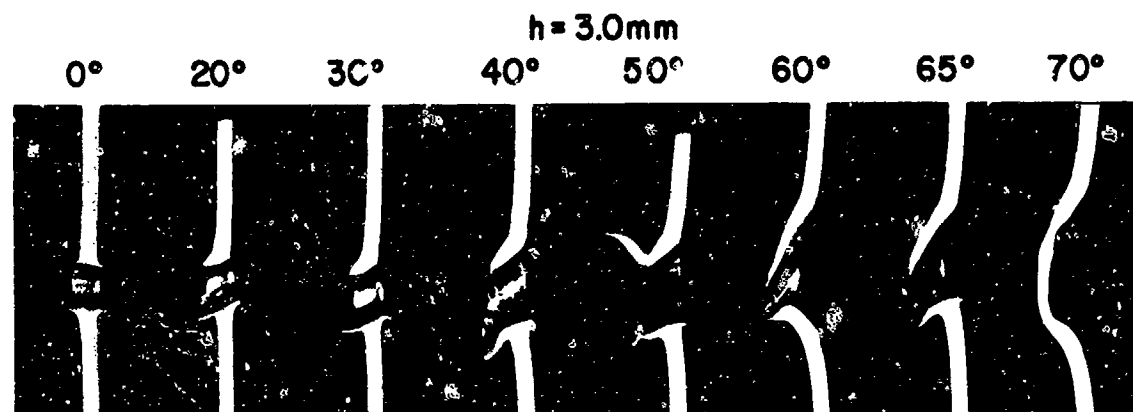
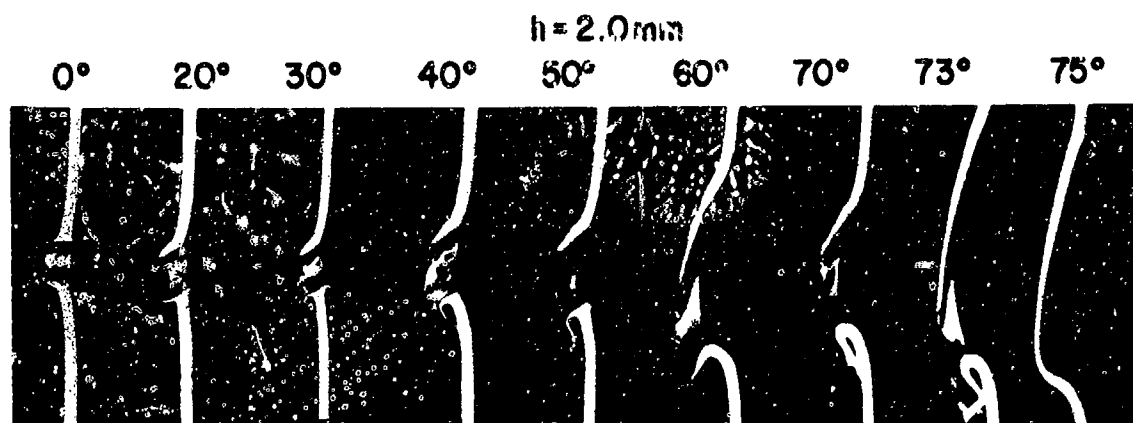


Fig.2



MATERIAL: COMMERCIAL PURE ALUMINUM

Fig. 3

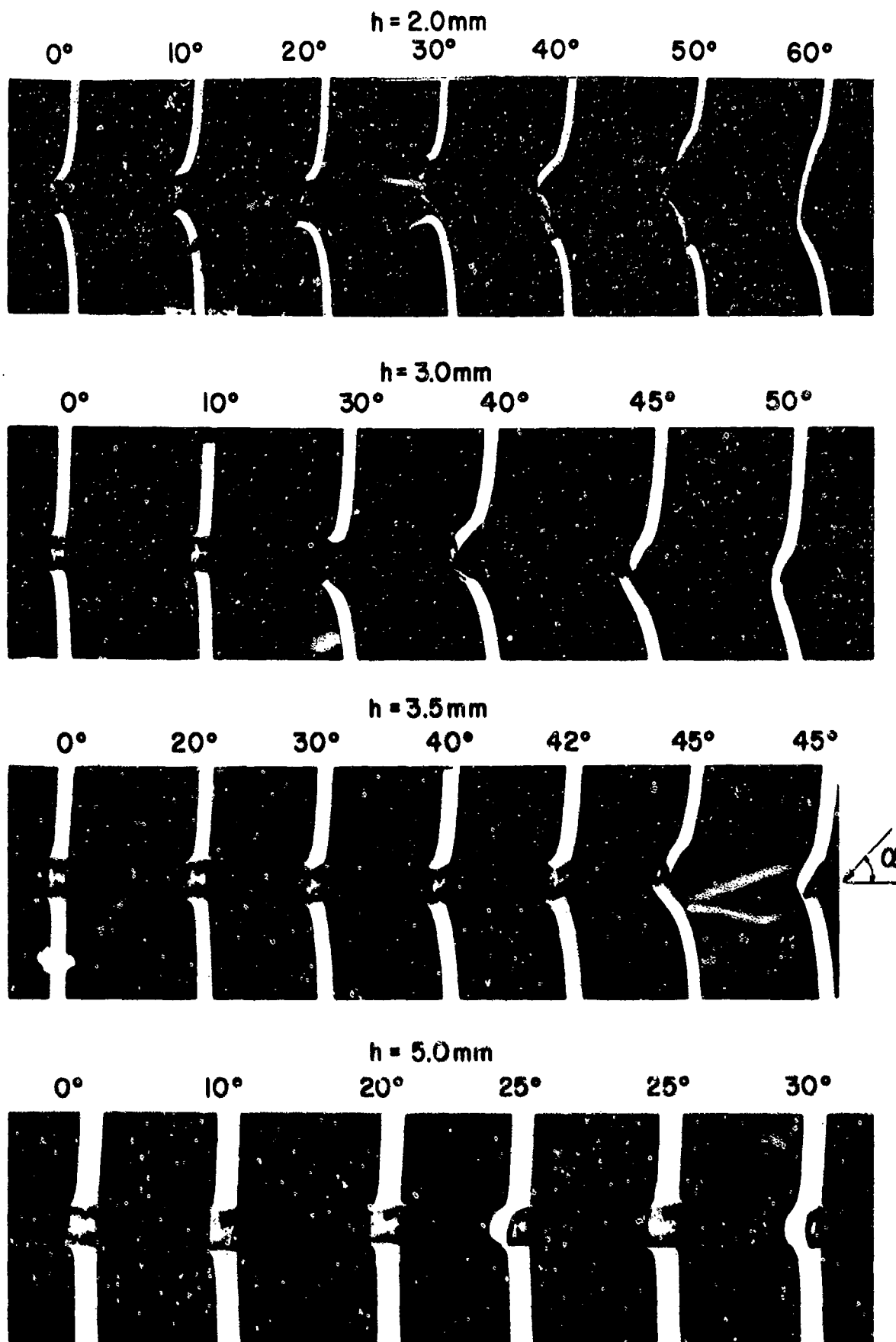


Fig. 4

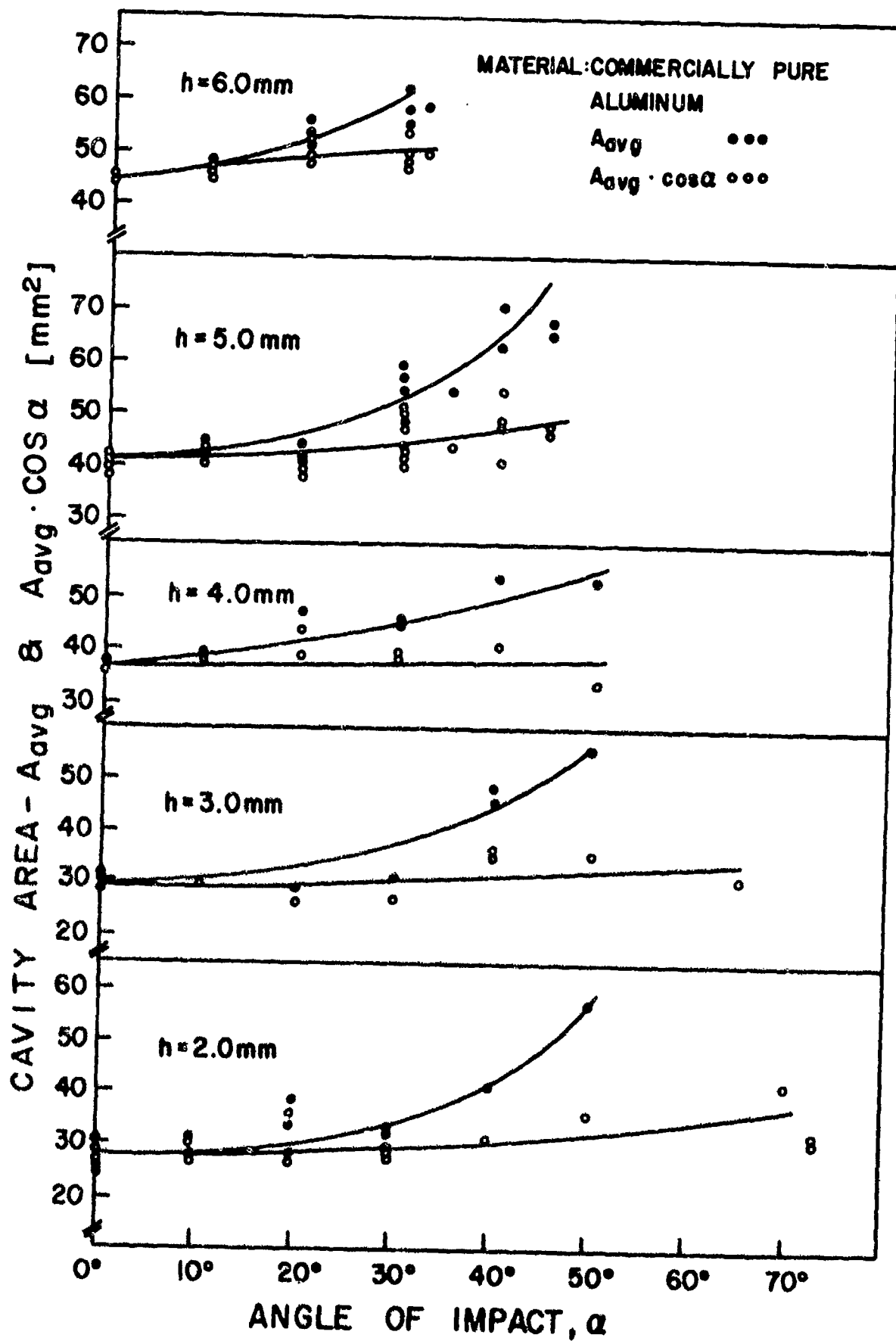


FIG.5

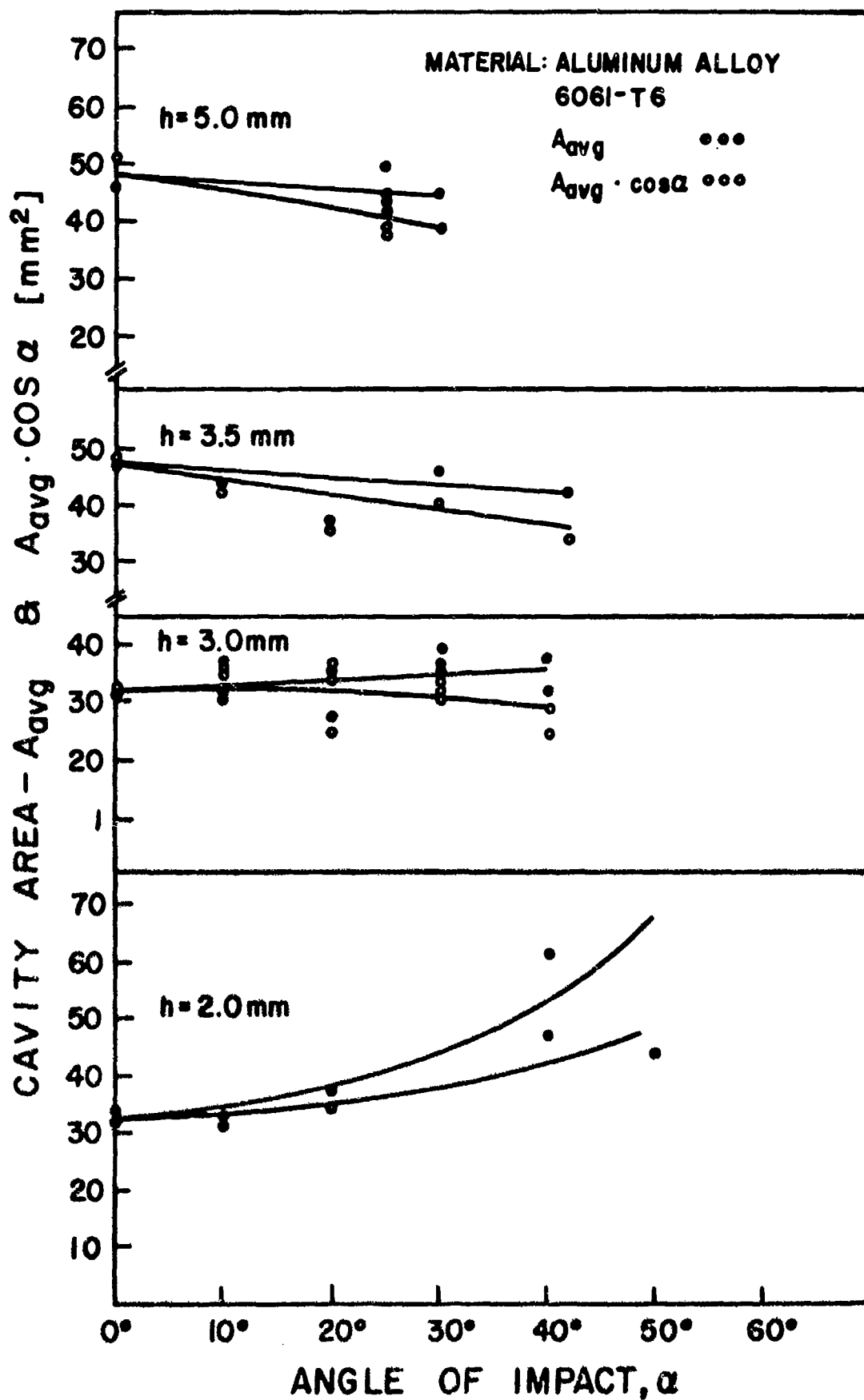


FIG. 6

COMMERCIALLY PURE ALUMINUM, $h = 5.0\text{mm}$; $\alpha = 30^\circ$

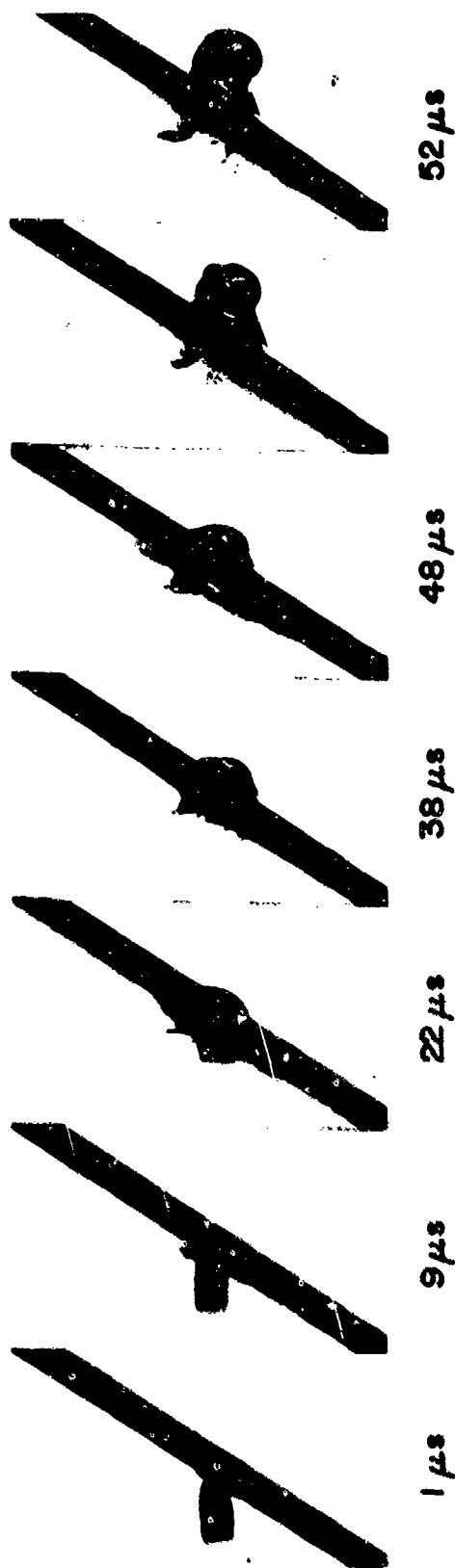


Fig. 7

ALUMINUM ALLOY 6061-T6, $h = 3.0\text{mm}$; $\alpha = 30^\circ$

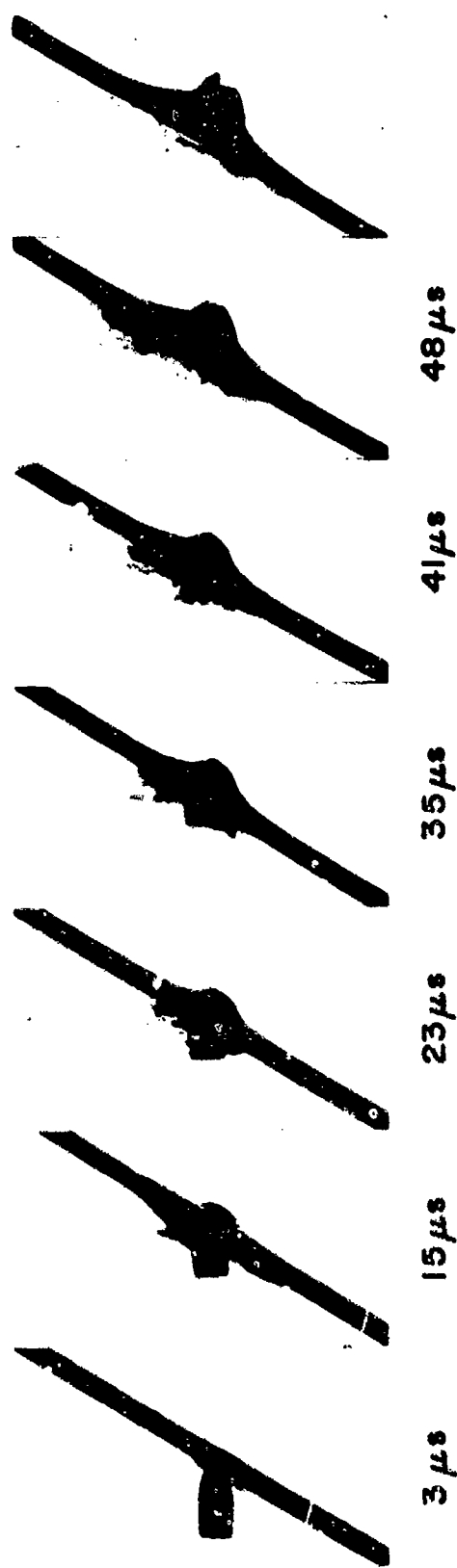
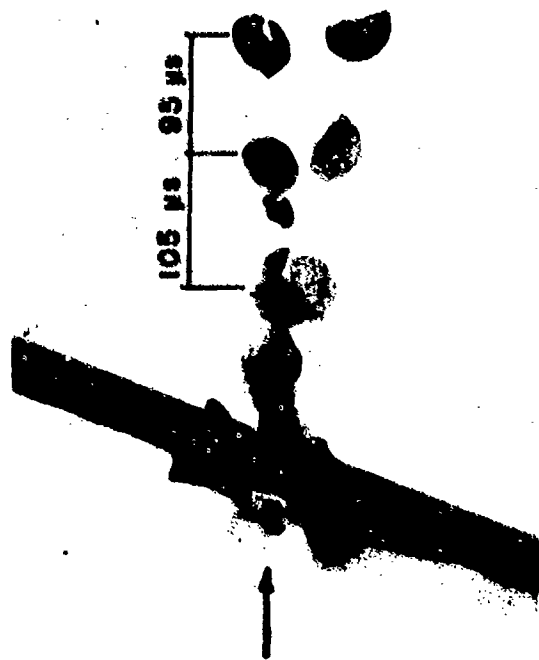


Fig. 8

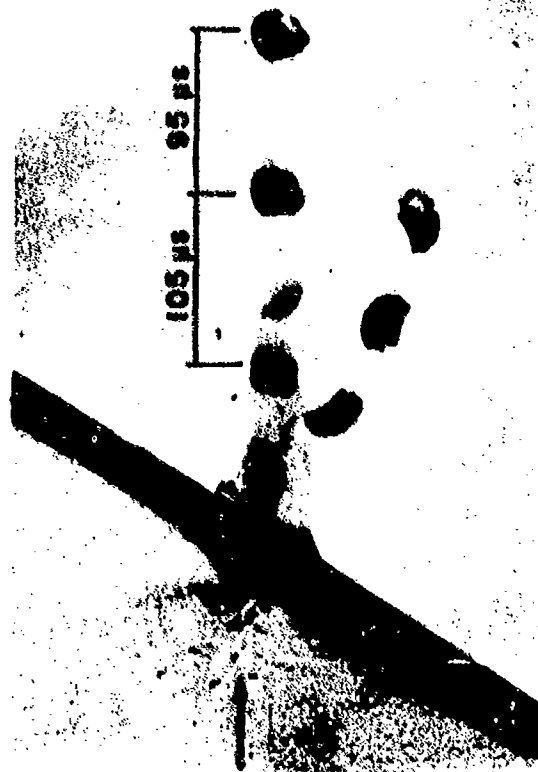
COMMERCIALY PURE ALUMINUM, $h=6.0\text{mm}$; $\alpha=20^\circ$



COMMERCIALY PURE ALUMINUM, $h=6.0\text{mm}$; $\alpha=30^\circ$



COMMERCIALY PURE ALUMINUM, $h=5.0\text{mm}$; $\alpha=30^\circ$



ALUMINUM ALLOY 6061-T6, $h=3.0\text{mm}$; $\alpha=30^\circ$

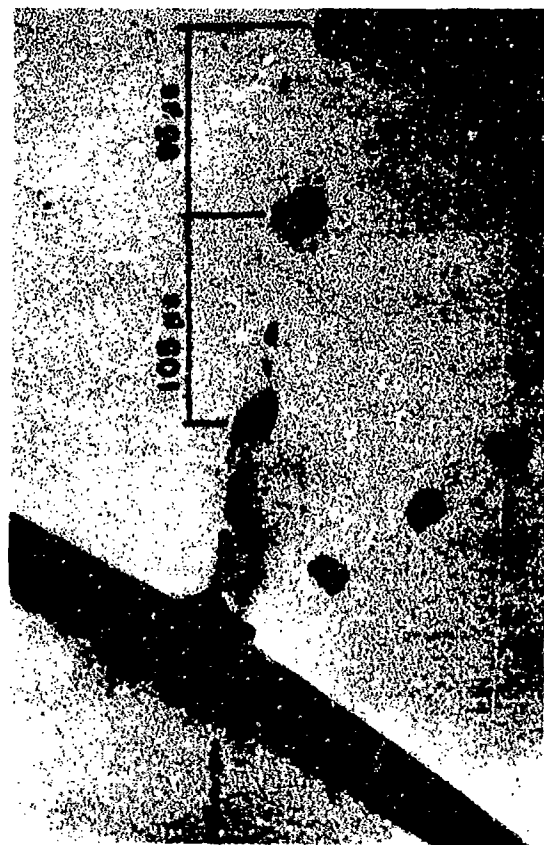


Fig. 9

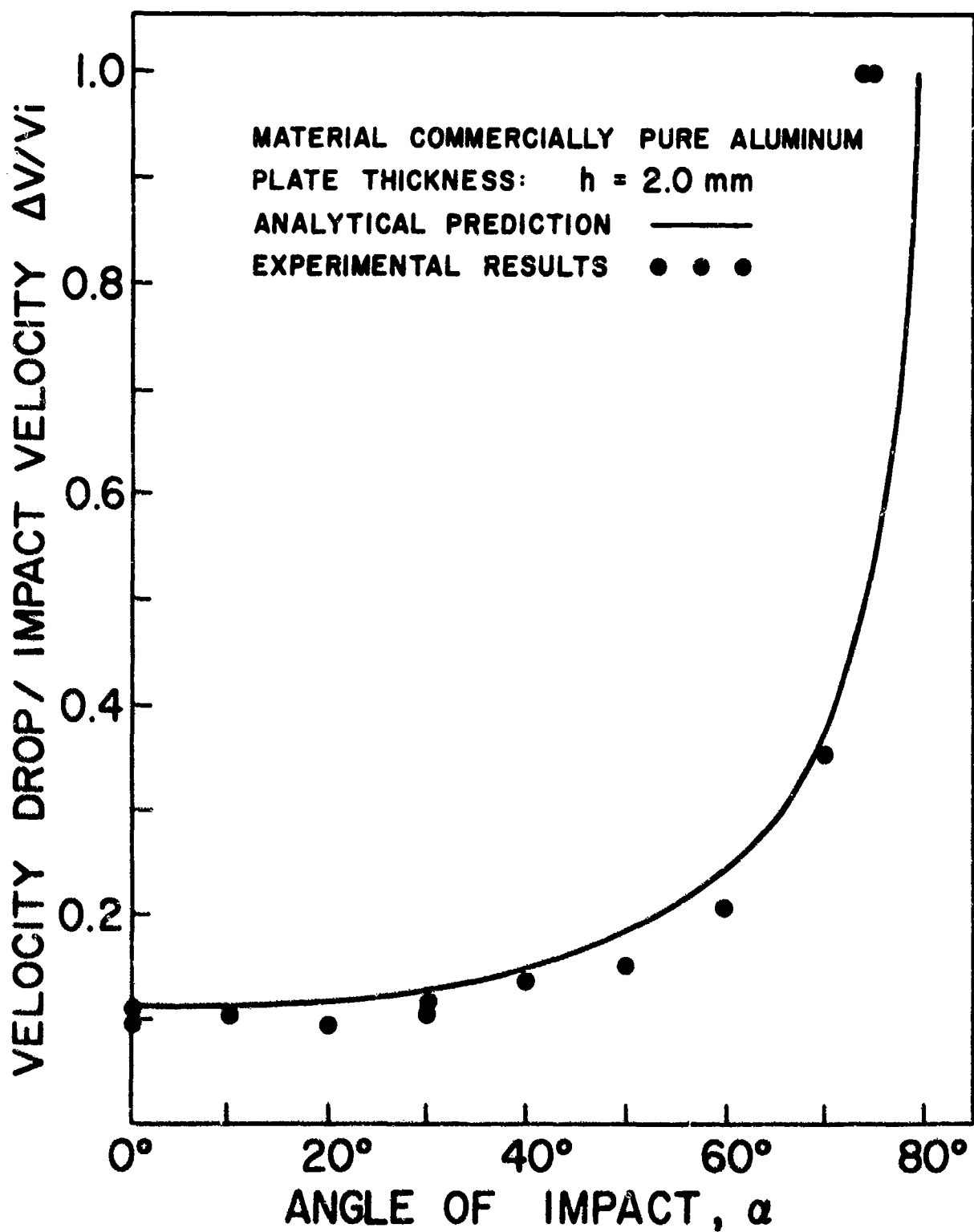


FIG.10

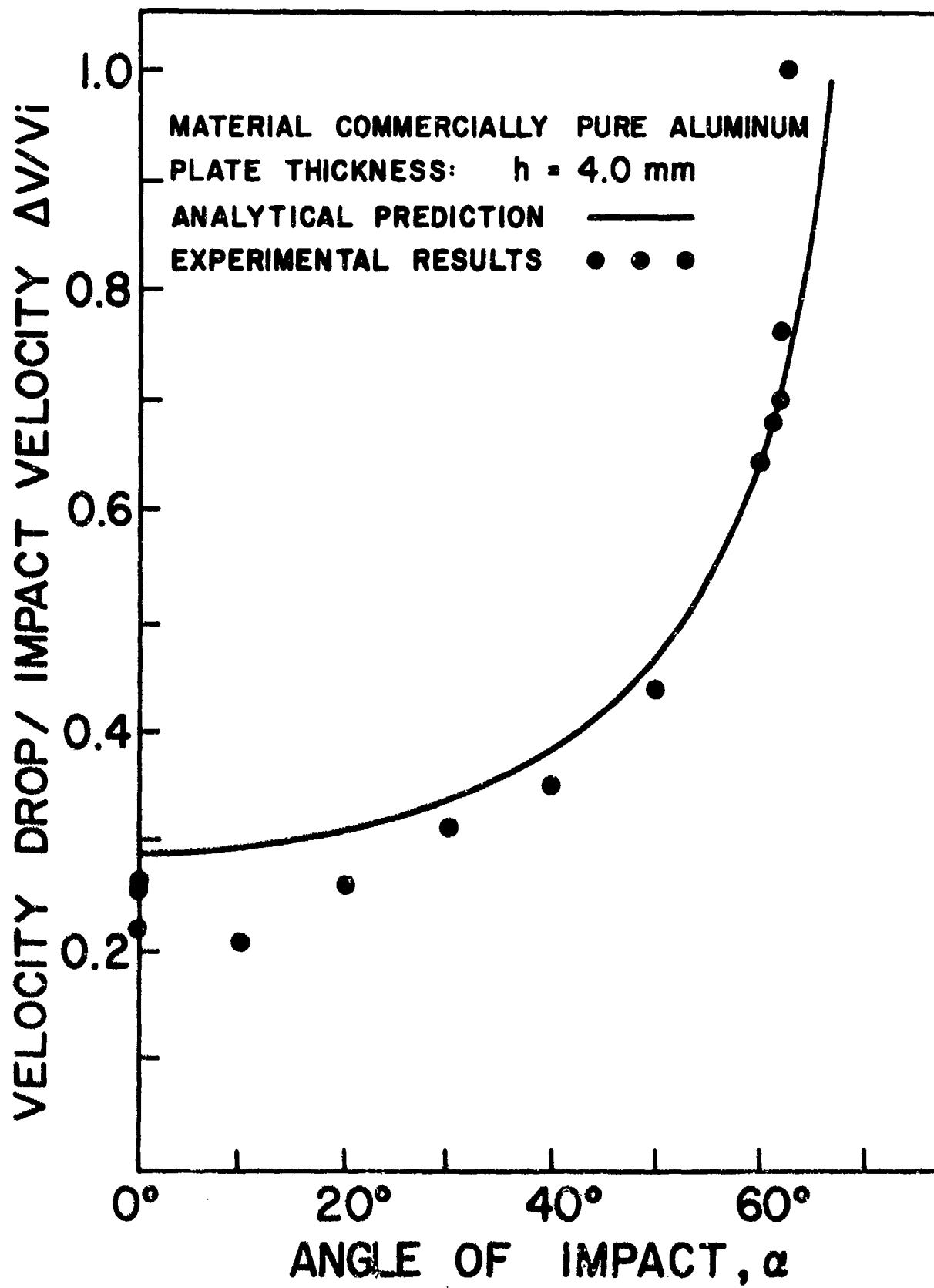


FIG. II

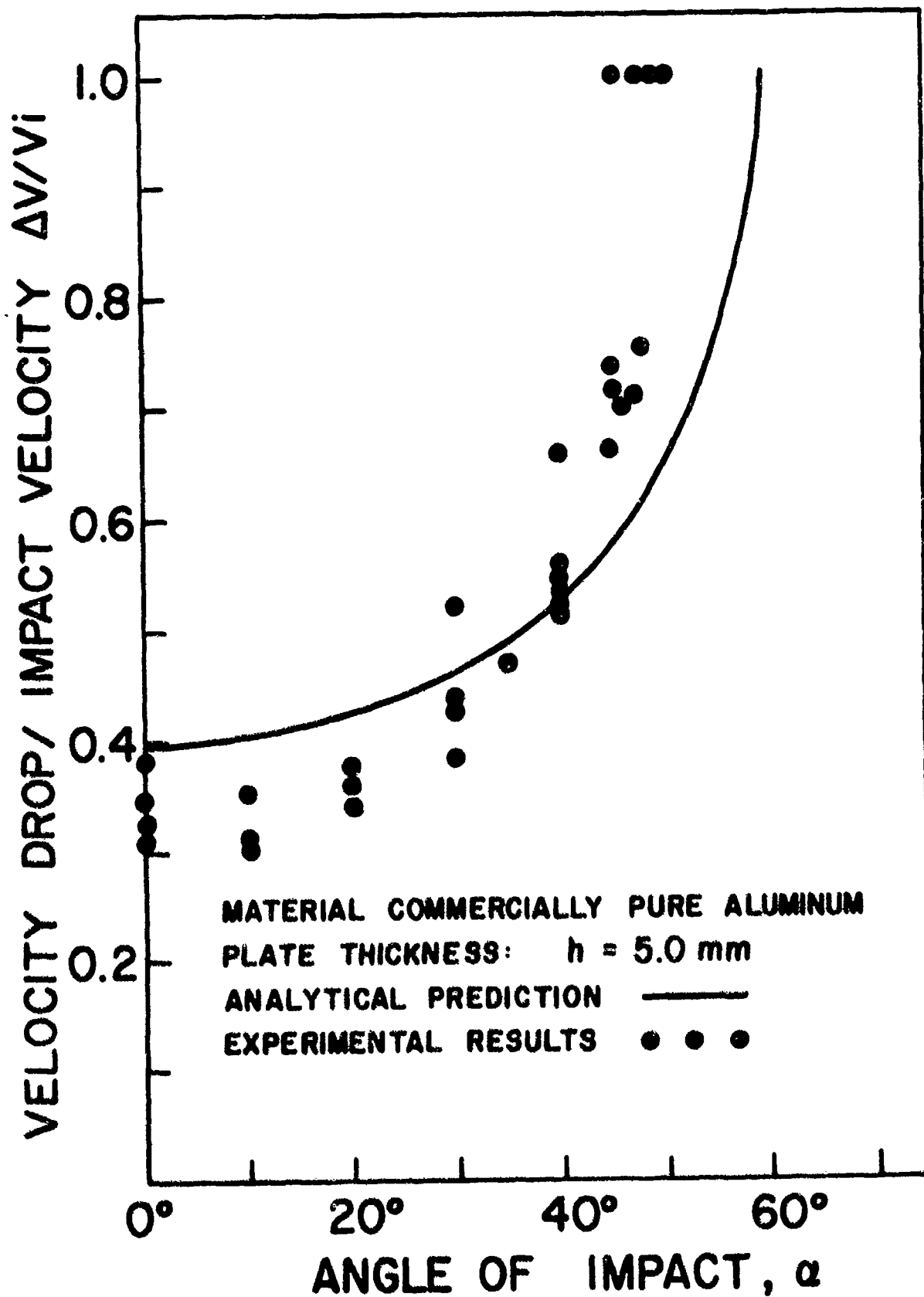


FIG.12

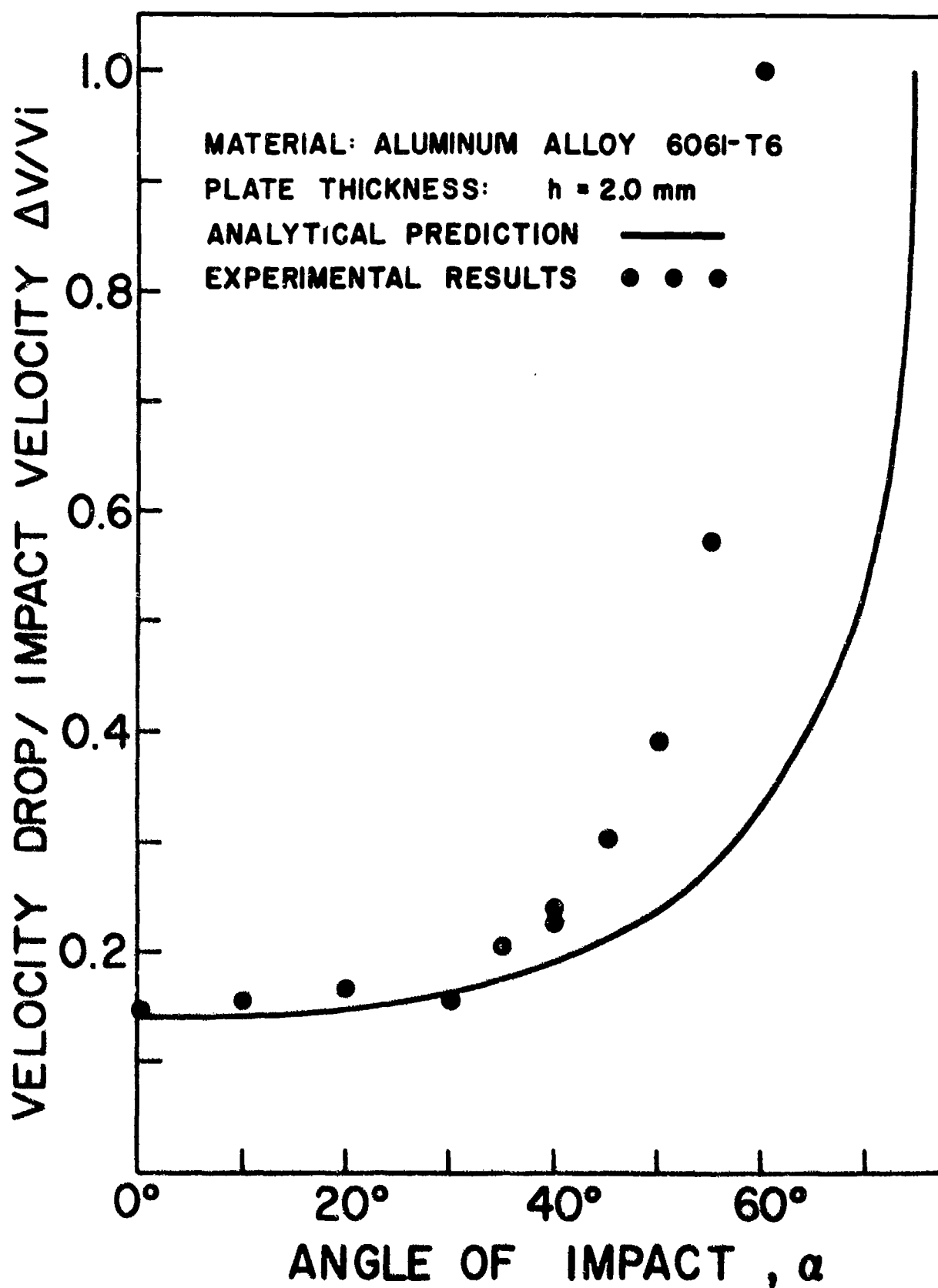


FIG. 13

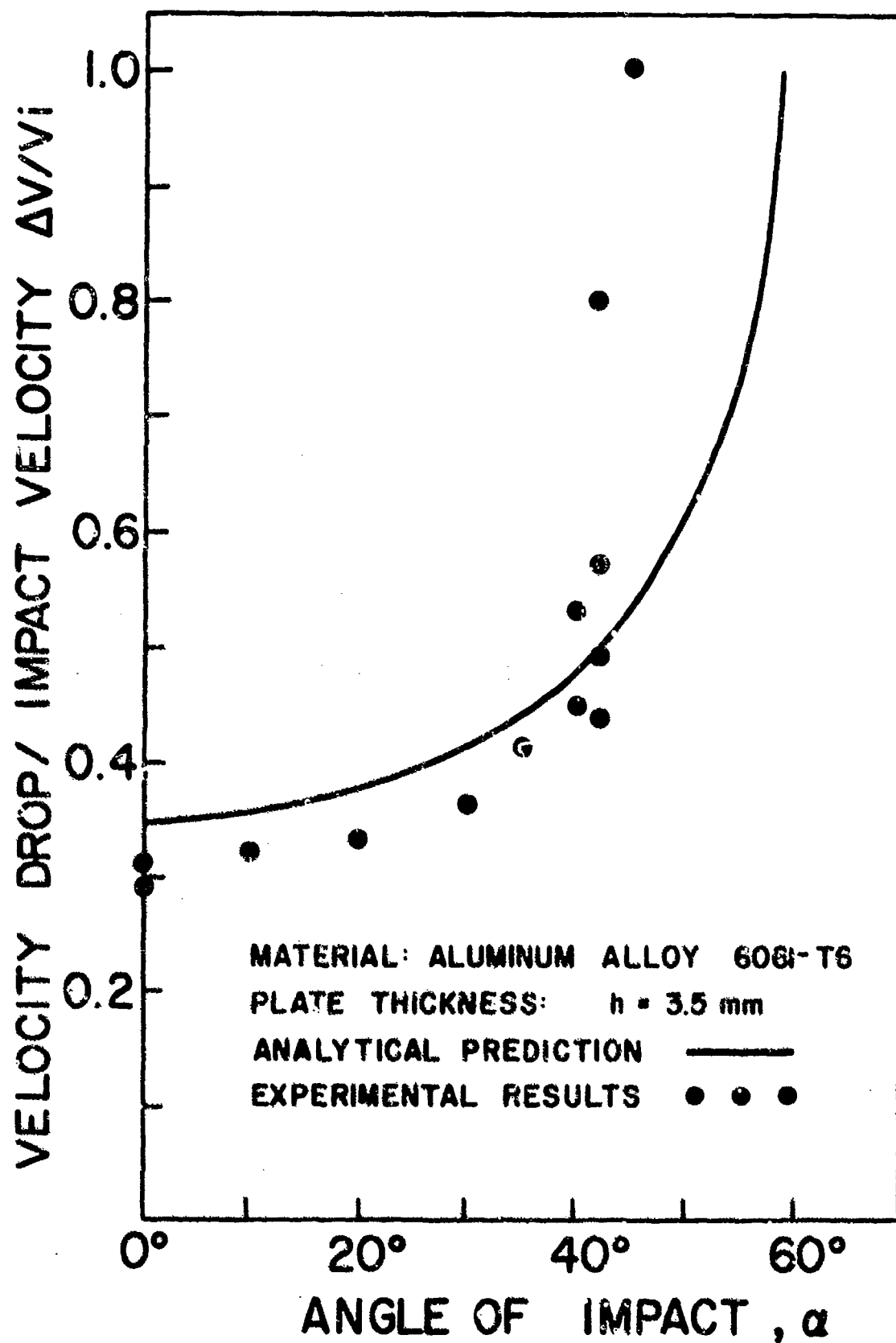


FIG.14

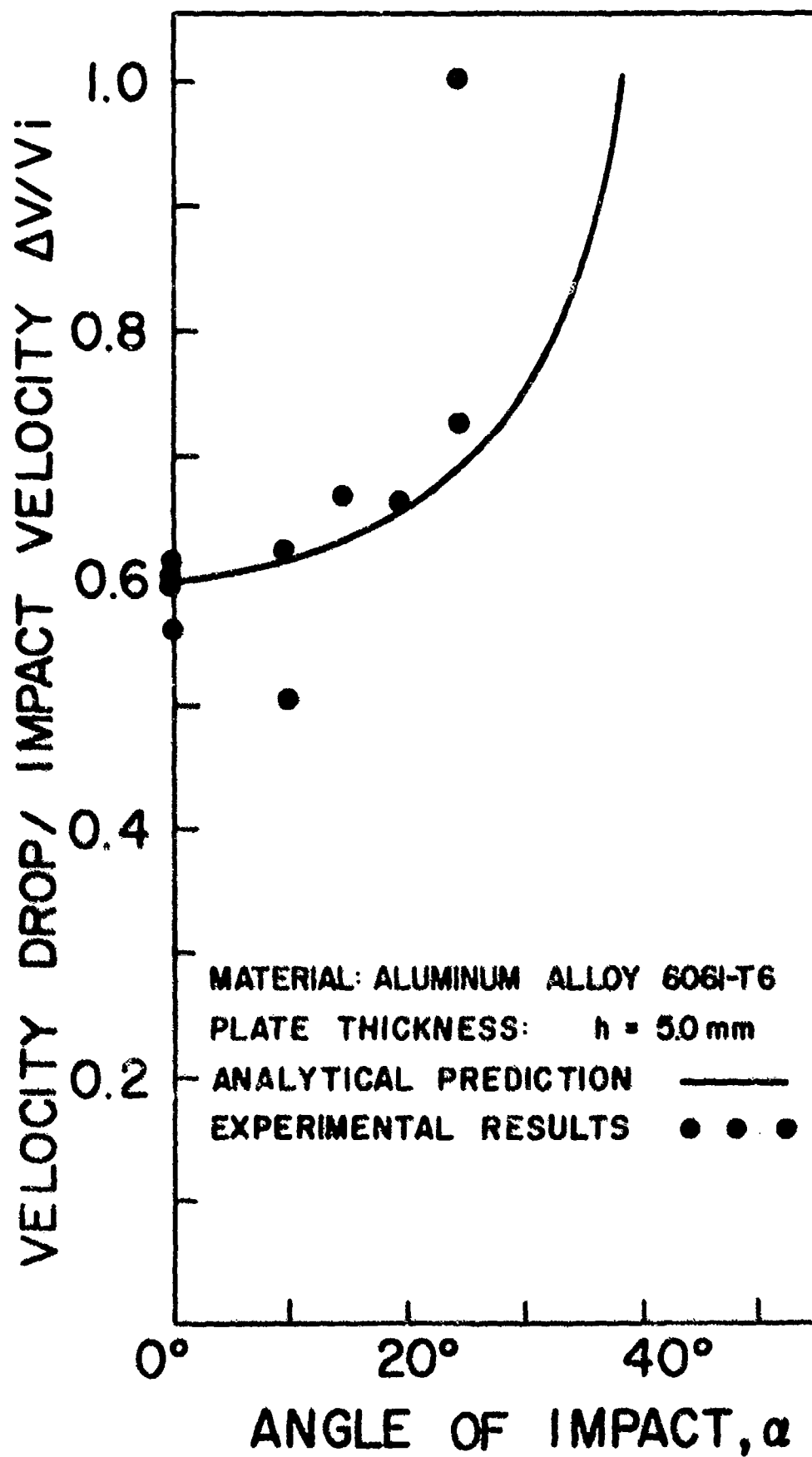


FIG. 15